

Simulation Study for Adsorption of Carbon Dioxide and Methane in Carbon-nanotubes

P. Phadungbut, W. Julklang, P. Sriling, W. Intomya, A. Wongkoblap* and
C.Tangsathitkulchai

School of Chemical Engineering, Institute of Engineering,
 Suranaree University of Technology, Nakhon Ratchasima, 30000, Thailand
 *E-mail: atichat@sut.ac.th

Manuscript received October 2, 2012
 Revised November 9, 2012

ABSTRACT

This paper presents the study of either carbon dioxide or methane adsorption in single wall carbon nanotube bundles (SWCNs) using a Monte Carlo simulation. Effects of tube diameter, tube wall distance and temperature on adsorption of each fluid in SWCNs are investigated. The adsorption capacity of fluid in a smaller tube diameter is greater than that in a larger pore diameter which observed at the same temperature, and tube wall distance, the initial adsorption occurs inside cylindrical pores. For the effect of separation spacing, an early onset in adsorption isotherm is observed for the smaller tube wall distances. In the case of 16.3 Å pore, if the wall distance is greater than 7 Å the adsorption initially occurs in the cusp interstices, on the other hand, it initially resides inside tubes. Finally the experimental data show that gas can be adsorbed in carbon nanotubes better than in activated carbon.

Keywords: Computer simulation, Carbon-nanotubes, Gas adsorption, Monte Carlo.

1. INTRODUCTION

Physical and chemical adsorptions on porous materials such as zeolite, activated carbon, polymeric materials and carbon nanotubes, plays an important role in many industries, and it is involved in many applications, including purification of gases and liquids, membrane technology, catalysis, energy storage and environmental technology. Single wall carbon nanotubes (SWCNs) have been increasingly used in many applications, for example methane and hydrogen storages, sensor technology and medical technology

since the discovery of carbon nanotubes by Iijima in 1991 [1]. SWCNs can stick to each other and form bundles due to the strong Van der Waals interactions [2]. As a result adsorption of fluids can occur outside SWCNs at the cusp interstices where the fluid-solid interaction potentials are enhanced to give the deepest potential minimum [3]. The characterization of the porosity of SWCNs and the adsorption mechanism of fluids in nanotube bundles are important for all applications.

Adsorption of carbon dioxide (CO_2) and methane (CH_4) has been of significant interest to adsorption science and engineering because carbon dioxide is a good molecular probe for characterizing the narrow micropores at experimentally measurable pressures [4] while methane adsorption is used to develop the new adsorbent for methane storage as a vehicular fuel. SWCNs are one of the promising adsorbents for methane storage. In addition, carbon dioxide and methane are implicated as greenhouse gases that can cause global warming due to greenhouse effects, therefore the utilization and reduction of greenhouse gases is becoming more important. To elucidate the adsorption mechanism of these fluids in carbon nanotubes, molecular simulation such as Monte Carlo (MC) and Molecular Dynamics (MD) should be used.

This study focuses on using homogeneous nanotubes bundles to investigate the adsorption mechanism of either CO_2 or CH_4 in single wall carbon nanotubes (SWCNs). The adsorption isotherms and snapshots of fluid at various temperatures are obtained by using a Grand Canonical Monte Carlo (GCMC) simulation. The effects of tube diameter (TD), tube wall distance (TWD) and temperature on the adsorption of these fluids will be investigated to determine the adsorption behavior.

2. METHODOLOGY

The Grand Canonical Monte Carlo simulation is used to obtain the adsorption isotherm for CH_4 and CO_2 adsorption in single wall carbon nanotube bundles at 273 and 300K. For this method to give correct results, the choice of fluid and solid models used in the simulation method is important. The essential equations used in the simulation are the potential equations between fluid particles and those between a fluid particle and a solid surface.

2.1 Solid Model

The solid model used in this study is the carbon-based adsorbents whose pores are cylinders. The simplest model of carbon nanotube as an isolated single cylinder has been commonly used in many studies; however it does not represent experimental carbon nanotubes because these tubes are usually found in tangled or partly aligned bundles [5]. In this study, carbon nanotubes bundle consisted of seven cylindrical tubes arranged in a hexagonal pattern, one at the center and the others arranged at the vertices of a hexagon is used as a solid model. Fig. 1 shows a schematic diagram of SWCNs bundle, each cylinder consists of one graphene wall and its diameter (TD) is that of a ring passing through the centers of the carbon layer. The separation spacing of carbon atoms on the external surface of two adjacent nanotubes is denoted as s . Tube diameters used in this paper are 9.5, 10.8, 13.6 and 16.3 Å and tube wall distances (s or TWD) are 4, 7 and 10 Å with 50 Å tube length.

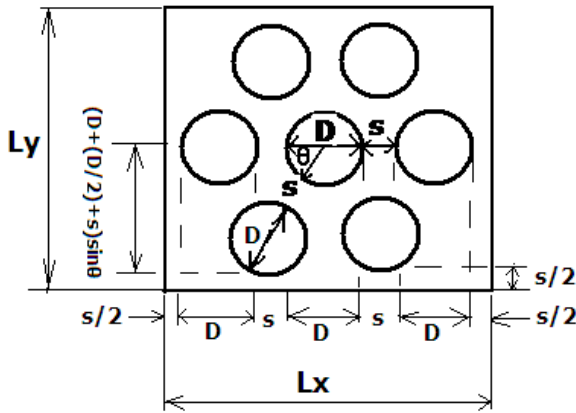


Fig. 1A Schematic Diagram of SWCNs Bundle Inside a Simulation Box.

2.2 Fluid Models

In this study, methane is modeled as a spherical and non-polar molecule with a single Lennard-Jones (LJ) center, although its molecular shape should be tetrahedral. This is due to the weak point charges of methane. The molecular parameters of methane, collision diameter and energy well depth, are $\sigma_{ij} = 3.73 \text{ \AA}$ and $\epsilon_{ij}/k = 148.0 \text{ K}$, respectively. While the molecular shape of carbon dioxide is linear structure with 3-LJ centers [6] and its parameters used in this study are shown in Table 1. The interaction energy between fluids is calculated using the Lennard-Jones 12-6 equation.

$$\phi_{ij} = 4\epsilon_{ij} \left[\left(\frac{\sigma_{ij}}{r_{ij}} \right)^{12} - \left(\frac{\sigma_{ij}}{r_{ij}} \right)^6 \right] \quad (1)$$

which r_{ij} is separation distance between fluids.

In the case of carbon dioxide, an electrostatic interaction between two point charges, each of which is on different molecule, is calculated by using the Coulomb's law.

$$\phi_{q^iq^j} = \frac{1}{4\pi\epsilon_0} \cdot \frac{q^i q^j}{r_{ij}} \quad (2)$$

where ϵ_0 is the permittivity of free space, r_{ij} is the distance between two charges.

Table 1 Molecular Parameters for CO_2 Molecule

parameter	value	parameter	value
^{c-c} σ	2.757 Å	^{c-c} ϵ/k	28.129 K
^{o-o} σ	3.033 Å	^{o-o} ϵ/k	80.507 K
^c q	0.6512e	^o q	-0.3256e
^{c-o} λ	1.149 Å		

2.3 Simulation Method

The GCMC with metropolis algorithm which specified temperature, volume and chemical potential of system is used to obtain the adsorption isotherm of fluids in a bundle of seven tubes [7]. One GCMC cycle consists of one thousand random moves with the equal probability of insertion, deletion and displacement moves. 20,000 GCMC cycles are used for the system to reach equilibrium, and additional 20,000 cycles are used to obtain ensemble averages. Each point of adsorption isotherm, an empty box is used as the initial configuration, and the simulation is carried out until the

number of particles in the box does not change.

The simulation box is a rectangular box which the dimension in the x and y axis depend on tube diameter and tube wall distance (L_x and L_y) while the z dimension being the same as the tube length (L). Box length in x axis can be calculated from:

$$L_x = 3(D + s) \quad (3)$$

In y direction, the distance from the center of the middle tube to the tube wall of adjacent tube along radius direction is equal to $D + (D/2) + s$. When we project it in y direction, it will be equal to $(D + (D/2) + s)\sin\theta$, where θ is $\pi/3$ radians. So the total length in y direction (L_y) is twice this length plus the two spacing between tube wall and simulation box.

$$L_y = 2 \left\{ \left(D + (D/2) + s \right) \sin\left(\frac{\pi}{3}\right) \right\} + 2 \left(\frac{s}{2} \right) \quad (4)$$

$$L_y = 2 \left\{ \left(\frac{3D}{2} + s \right) \sin\left(\frac{\pi}{3}\right) \right\} + s$$

The average pore density can be defined as the ratio of fluid particles or molecules inside the pores to pore volume:

$$\rho = \frac{N_{\text{inside}}}{V_{\text{pore}}} \quad (5)$$

$$V_{\text{pore}} = 7\pi(R - \sigma_{ss})^2 L \quad (6)$$

which R is tube radius and σ_{ss} is collision diameter between carbon atoms which equals to 0.34 nm and L is carbon nanotube length. While the average bulk density is defined as the ratio of the number of particle outside the pores to volume of simulation box, where box volume is defined as $L_x L_y L - V_{\text{pore}}$, and N_{outside} is defined as $N - N_{\text{inside}}$, where N is total number of particle.

3. RESULTS AND DISCUSSIONS

In this paper, first, we start our discussion by presenting the effects of pore diameter on the adsorption isotherm of CH_4 and CO_2 in carbon nanotubes bundle at 273K. Then we discuss the effects of the separation spacing on the adsorption isotherm. Next the effects of temperature are studied, and finally experimental adsorption isotherms of CO_2 at 273K obtained for activated carbon and carbon nanotubes will be compared.

3.1 Effects of Tube Diameter on Adsorption Isotherm

The simulated isotherms versus pressure for CH_4 and CO_2 in bundle of SWCNs with a tube wall distance of 7 Å at 273K for 10.8 and 16.3 Å tubes are shown in Fig.2. The snapshots of CO_2 and CH_4 in tube diameter of 10.8 Å are shown in Fig. 3 and Fig. 4, respectively to show the preferential adsorption at low loadings. First, we will discuss the effect of tube diameter on CH_4 and CO_2 adsorption and then compare the adsorption mechanism between both adsorbates.

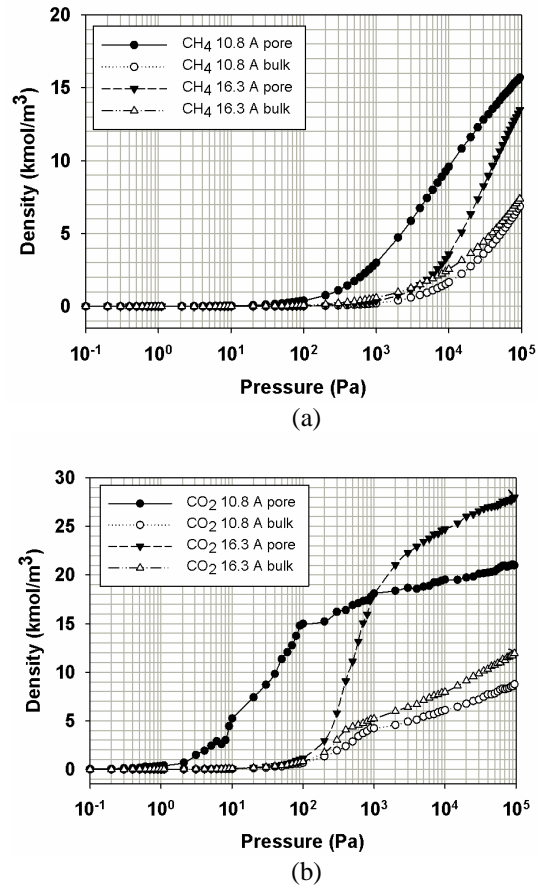


Fig.2 Adsorption Isotherms of (a) CH_4 and (b) CO_2 in Bundles of Tube Size 10.8 and 16.3 Å with Tube Wall Distance of 7 Å at 273 K.

Adsorption isotherms of CH_4 and CO_2 in bundles of carbon nanotubes of different sizes are shown in Fig. 2(a) and (b), respectively, the similar behavior for the bundles of smallest tubes (10.8 Å) and those of larger tubes (16.3 Å) can be observed. At low pressures, fluid molecules are initially adsorbed in the interior of the tubes to form a monolayer because of the stronger solid-fluid potential inside the tube. The snapshots in Fig. 3

(a) and (b) for CO_2 adsorption and Fig. 4 (a) – (c) for CH_4 adsorption show this preferential adsorption inside the tube. As pressure is increased adsorption continues to occur inside the tube and adsorption begins to happen in the various interstices outside the tubes as shown in Fig. 3 (c) – (e) and Fig. 4 (d) – (e). The initial adsorption pressure for the bundles of larger tubes is greater than that for those of smaller tubes. This is due to the stronger interaction between fluid and solid in the case of smaller tubes. The following features are also observed: (i) the adsorption density inside the tube increases gradually with pressure due to the molecular layering and the pore-filling mechanisms and (ii) the density outside the tube also increase gradually. The adsorption isotherm outside the tube for larger and smaller tubes with narrow TWD are not much different, this is due to that the interstices between tubes can be packed with one layer as one can seen from Fig. 3 (c) and 4 (d) for CO_2 and CH_4 , respectively.

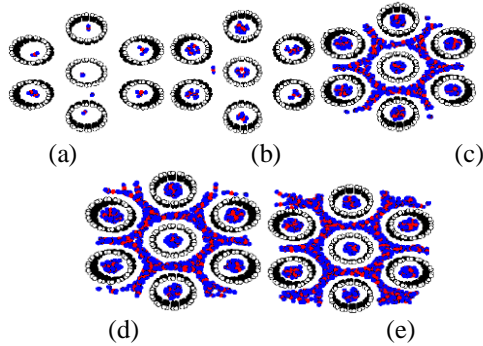


Fig. 3 Snapshots of CO_2 Adsorption at Various Pressures: (a) $P = 0.3$, (b) 1, (c) 900, (d) 8000 and (e) 90000 Pa in 10.8 \AA Tubes at 273K and TWD of 7 \AA .

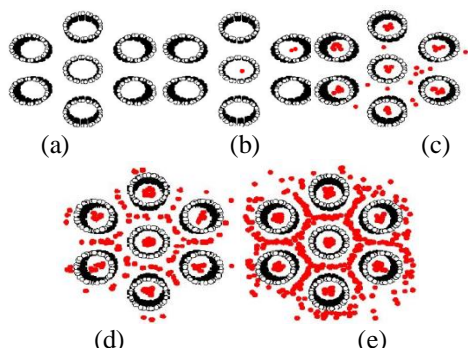


Fig. 4 Snapshots of CH_4 Adsorption at Various Pressures: (a) $P = 0.3$, (b) 1, (c), 900, (d) 8000 and (e) 90000 Pa in 10.8 \AA Tubes at 273 K and TWD of 7 \AA .

Now turn to the discussion of adsorption behavior between CH_4 and CO_2 in bundles of tubes, CO_2

molecules initially adsorb at lower pressures than those of CH_4 for the same tube diameter. At the same pressure and tube diameter, adsorption density inside the tube for CO_2 is greater than that for CH_4 and this is due to the quadrupole effect in the case of CO_2 and lead to the stronger fluid-solid interaction.

3.2 Effects of Tube Wall Distance

Having seen the effects of the tube diameter, now turn to discussing the effects of tube wall distance on adsorption mechanism. The simulation isotherms of CH_4 and CO_2 in bundles of SWCNs of 16.3 \AA at 273 K at various tube wall distance of 4, 7 and 10 \AA are shown in Fig. 5 while the snapshots of CH_4 adsorption in bundles of tubes for tube wall distance of 4 and 10 \AA are shown in Fig. 6 and 7, respectively.

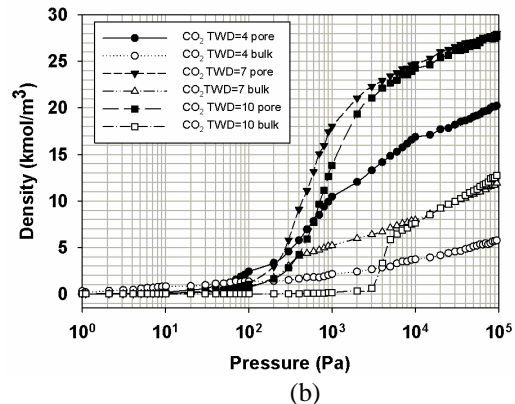
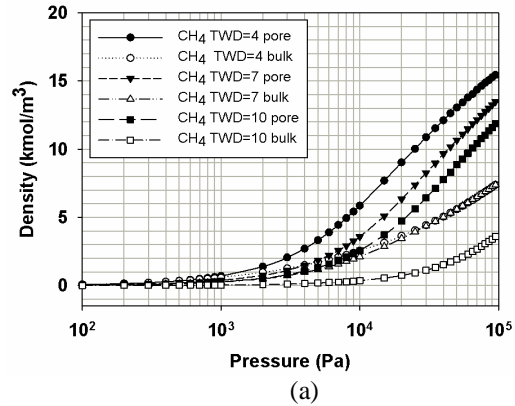


Fig. 5 Adsorption Isotherms of (a) CH_4 and (b) CO_2 in Bundles of 16.3 \AA Tubes at 273K at Various Tube Wall Distance of 4, 7 and 10 \AA .

Observing these isotherms for bundles of carbon nanotubes of different tube wall distances, the distinct difference between the tube wall distance less than 10 \AA

(4 and 7 Å) and TWD of 10 Å at low loadings can be observed. At low pressures, fluid particles are initially adsorbed inside the tubes if the separation spacing is less than 10 Å due to the stronger solid-fluid potential inside the tube as discussed in Section 3.1. The snapshots in Fig. 6 show this preferential adsorption inside the tube. For larger tube wall distance, the behavior is different from the TWD less than 10 Å tubes in that at low loadings adsorption occurs in the cusp interstices where the solid-fluid potential is stronger than that inside the tube (see the snapshots in Fig. 7). This is the direct result from the difference in size of the cusp interstices and the tube diameter. As a result, when the tube radius is greater than the separation spacing between tubes, adsorption in the cusp interstices occurs first followed by that in the tube interior. The opposite is true when the tube radius is smaller than the spacing [8]. In the case of CO₂ adsorption outside the tubes of 16.3 Å diameter and TWD of 10 Å, the isotherm increase gradually due to the layering outside the tube walls and then suddenly changes in adsorption isotherm. This is due to that the adsorption is the exothermic process and the adsorbed molecules acquire the greater energy to evaporate [9].

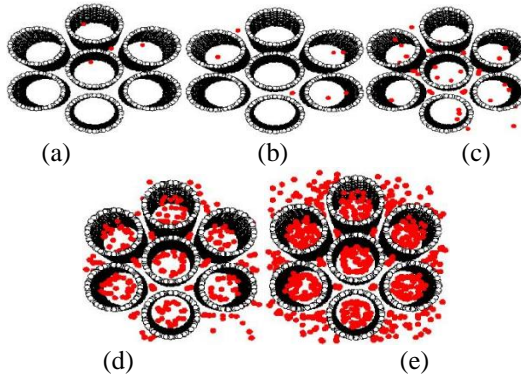


Fig. 6 Snapshots of CH₄ Adsorption in Bundles of 16.3 Å Tubes at 273K and TWD of 4 Å at (a) $P = 50$, (b) 200, (c) 1000, (d) 10000 and (e) 100000 Pa.

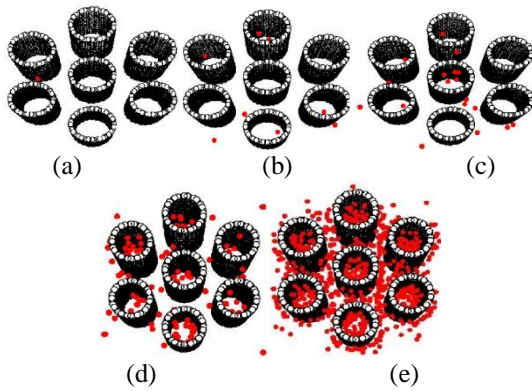


Fig. 7 Snapshots of CH₄ Adsorption in Bundles of 16.3 Å Tubes at 273K and TWD of 10 Å at (a) $P = 50$, (b) 200, (c) 1000, (d) 10000 and (e) 100000 Pa.

3.3 Effect of Temperature

Fig. 8 shows the results of CO₂ and CH₄ adsorptions in SWCNs with tube size of 9.5 Å and tube wall distance of 4 Å at 273 and 300K. The adsorption isotherm decreases by increasing temperature which usually observed in the physical adsorption. This is due to that the adsorption is the exothermic process and the adsorbed molecules acquire the greater energy to evaporate [9].

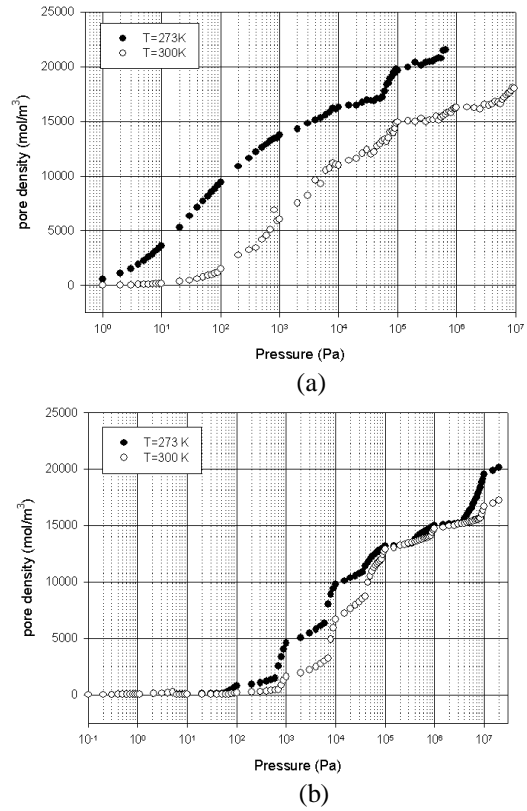


Fig. 8 Adsorption Isotherms of (a) CO₂ and (b) CH₄ at 273 and 300K in Bundles of Tube Size 9.5 Å and Tube Wall Distance of 4 Å.

3.4 Comparison between the Adsorption Isotherm for Activated Carbon and That for Carbon Nanotubes

The experimental results shown in Fig. 9 are obtained by using an Intelligent Gravimetric Analyzer (IGA) for the adsorption of CO₂ in Longan seed activated carbon produced in our laboratory and carbon

nanotubes at 273K. Prior to adsorption experiments, the carbon sample about 0.2 g is outgassed at 200°C for 10 hours, and then is cool down to the adsorption temperature. As seen in Fig. 9, the adsorbed amount of CO₂ in carbon nanotubes is greater than that in activated carbon. This is due to that carbon nanotubes have strong interaction according to their circular orientation of carbon atoms.

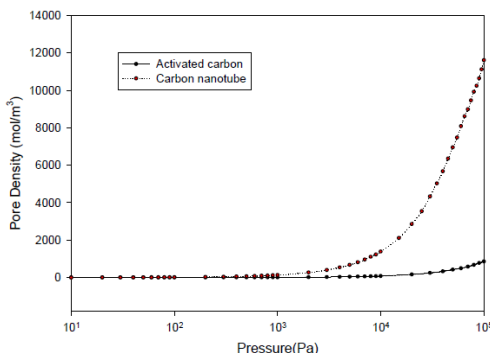


Fig. 9 CO₂ Adsorption Isotherms Obtained for Activated Carbon and Carbon Nanotubes at 273K.

4. CONCLUSION

In this paper, adsorption isotherms of CO₂ and CH₄ in nanotube bundles have been presented. The simulation results can be used to describe the adsorption behavior in carbon nanotubes. It has been found that tube diameter, tube wall distance and temperature affect the adsorption isotherm. For the smaller tubes, the adsorption initially occurs inside the tube interior however the initial adsorption is carried out at the cusp interstices if the tube radius is greater than the separation spacing. This study will lead to an understanding for CH₄ and CO₂ adsorption in carbon nanotubes and may be used for further study in energy storage and solid development for separating the exhaust gases mixture.

5. ACKNOWLEDGEMENTS

We acknowledge the Thailand Research Fund and the Commission on Higher Education for research funding to AW and Suranaree University of Technology for the financial support for presenting in the conference.

REFERENCES

- [1] S. Iijima, "Helical microtubules of graphitic carbon", *Nature*, Vol. 354, pp. 56, 1991.
- [2] S. Agnihotri, J.P.B. Mota, M. Rostam-Abadi, M.J. rood, *Carbon*, Vol. 44, pp. 2376, 2006.
- [3] K. Murata, K. Kaneko, W.A. Steele, F. Kokai, K. Takahashi, D. Kasuva, K. Hirahara, M. Yudasaka, S. Iijima, *J. Phys. Chem. B*, 105, pp. 10210, 2001.
- [4] P.I. Ravikovich, A. Vishnyakov, R. Russo, A.V. Neimark, "Unified Approach to Pore Size Characterization of microporous Carbonaceous Materials from N₂, Ar and CO₂ Adsorption Isotherms", *Langmuir*, Vol. 16, pp. 2311, 2000.
- [5] Y.F. Yin, T. Mays, B. McElaney, "Adsorption of Nitrogen in Carbon Nanotube Arrays", *Langmuir*, Vol. 15, pp. 8714, 1999.
- [6] J.G. Harris, K.H. Yung, "Carbon Dioxide's Liquid-Vapor Coexistence Curve and Critical Properties as Predicted by a Simple Molecular Model", *Journal of Physical Chemistry*, Vol.99, pp.12021-12024, 1995.
- [7] D. Frenkel, B. Smit, *Understanding Molecular Simulation*, 2nd edition, Academic Press, New York, 2002.
- [8] A. Wongkoblap, D.D. Do, K. Wang, "Adsorption of Polar and Nonpolar Fluids in Carbon Nanotube Bundles: Computer Simulation and Experimental Studies", *Journal of Colloid and Interface Science*, Vol. 331, pp.65-76, 2009.
- [9] D.D. Do, *Adsorption Analysis: Equilibria and Kinetics*, Imperial College Press, New Jersey, 1998.

P. Phadungbut, Biography not available at the time of publication.

W. Julklong, Biography not available at the time of publication.

P. Sriling, Biography not available at the time of publication.

W. Intomya, Biography not available at the time of publication.

A. Wongkoblap, Biography not available at the time of publication.

C. Tangsathitkulchai, Biography not available at the time of publication.